Calcium Induces Binding and Formation of a Spin-Coupled Dimanganese(II,II) Center in the Apo-Water Oxidation Complex of Photosystem II as Precursor to the Functional Tetra-Mn/Ca Cluster†

Gennady M. Ananyev and G. Charles Dismukes*

Princeton University, Hoyt Laboratory, Department of Chemistry, Princeton, New Jersey 08544

Received March 18, 1997; Revised Manuscript Received July 2, 1997⊗

ABSTRACT: Two new intermediates are described which form in the dark as precursors to the light-induced assembly of the photosynthetic water oxidation complex (WOC) from the inorganic components. Mn^{2+} binds to the apo-WOC−PSII protein in the absence of calcium at a high-affinity site. By using a hydrophobic chelator to remove Mn^{2+} and Ca^{2+} from the WOC and nonspecific Fe^{3+}, a new EPR signal becomes visible upon binding of Mn^{2+} to this site, characterized by six-line ^{55}Mn hyperfine structure ($\Delta H_{pp} = 96 \pm 1$ G) and effective $g = 8.3$. These features indicate a high-spin electronic ground state ($S = {}^5/_2$) for Mn^{2+} and a strong ligand field with large anisotropy. This signal is eliminated if excess Ca^{2+} or Mg^{2+} is present. A second Mn^{2+} EPR signal forms in place of this signal upon addition of Ca^{2+} in the dark. The yield of this Ca-induced Mn signal is optimum at a ratio of 2 Mn/PSII, and saturates with increasing $[Ca^{2+}] \geq 8$ mM, exhibiting a calcium dissociation constant of $K_D = 1.4$ mM. The EPR signal of the Ca-induced Mn center at 25 K is asymmetric with major g value of ≈2.04 ($\Delta H_{pp} = 380$ G) and a shoulder near $g \approx 3.1$. It also exhibits resolved ^{55}Mn hyperfine splitting with separation $\Delta H_{pp} = 42-45$ G. These spectral features are diagnostic of a variety of weakly interacting Mn_2(II,II) pairs with electronic spins that are magnetic dipolar coupled in the range of intermanganese separations 4.1 ± 0.4 Å, and commonly associated with one or two carboxylate bridges. The calcium requirement for induction of the Mn_2(II,II) signal matches the value observed for steady-state O_2 evolution (Michaelis constant, $K_M \approx 1.4$ mM), and for light-induced assembly of the WOC by photoactivation. The Ca-induced Mn_2(II,II) center is a more efficient electron donor to the photooxidized tyrosine radical, Tyr_Z^+, than is the mononuclear Mn center present in the absence of Ca^{2+}. The Ca-induced Mn_2(II,II) signal serves as a precursor for photoactivation of the functional WOC and is abolished by the presence of Mg^{2+}. Formation of the Mn_2(II,II) EPR signal by addition of Ca^{2+} correlates with reduction of flash-induced catalase activity, indicating that calcium modulates the accessibility or reactivity of the Mn_2(II,II) core with H_2O_2. We propose that calcium organizes the binding site for Mn ions in the apo-WOC protein and may even interact directly with the Mn_2(II,II) pair via solvent or protein-derived bridging ligands.

The atomic structure of the manganese and calcium sites of the photosynthetic water oxidation complex (WOC)[1] required for water oxidation and oxygen evolution remain unsolved puzzles of the PSII protein complex. Structural and functional clues have come from a number of different sources. There is a wide agreement on the presence of four Mn/WOC in the functional enzyme, although the number varies with the type of preparation and its source [for a review see Debus (1992) and Britt (1996)]. Recently, it has been found from titration studies that precisely 4.0 Mn/RC PSII bind cooperatively to the apo-WOC with restoration of O_2 evolution activity during the process of photoactivation (Ananyev & Dismukes, 1995, 1996a). Also, the "multiline" EPR signals at $g = 2$ (MLS) found in the S_2 state of intact WOC are now generally accepted as due to ^{55}Mn hyperfine coupling minimally within a tetramanganese core (Dismukes, 1991; dePaula et al., 1986; Bonvoisin et al., 1992; Kusunoki, 1992; Yachandra et al., 1996), although see Ahrling and Pace (1995). EPR spectral simulations support a stoichiometry of four Mn ions and further identify the responsible oxidation states as Mn(III) and Mn(IV) (Bonvoisin et al., 1992; Zheng & Dismukes, 1996; Kusunoki, 1992; Randall et al., 1995).

A different EPR signal forms at $g = 4.1$ in place of the MLS in samples treated by various reversible methods that produce an altered S_2 configuration (Casey & Sauer, 1984; Zimmermann & Rutherford, 1984, 1986). This spectral form is now known to arise from near-infrared illumination of the S_2 MLS state, possibly by direct absorption by the WOC (Boussac et al., 1996) and also by chloride depletion or $Cl^- \leftrightarrow F^-$ exchange. The signal has been suggested to arise from a single Mn(IV) ion that is uncoupled from the original Mn tetramer (Lei & Kramer, 1988), a Mn tetramer (dePaula & Brudvig, 1985) or possibly a rhombic Mn(II) monomer or

† This work was supported by the National Institutes of Health (Grant GM39932).

* To whom correspondence should be addressed. FAX: (609) 258-1980. E-mail: dismukes@chemvax.princeton.edu.

⊗ Abstract published in *Advance ACS Abstracts,* September 1, 1997.

[1] Abbreviations: apo-WOC-PSII, BBY membrane fragments after 20−35 mM TPDBA treatment; Chl, chlorophyll; DCBQ, 2,5-dichloro-*p*-benzoquinone; DCIP, 2,6-dichlorophenolindophenol; HFS, hyperfine structure; LED, light-emitting diode; MES, 2-(*N*-morpholino)ethanesulfonic acid; P680, primary electron donor; PSII, photosystem II; Pheo, primary pheophytin electron acceptor of PSII; Q_A and Q_B, primary and secondary plastoquinone electron acceptors; RC, reaction center; TPDBA, *N*,*N*,*N*′,*N*′-tetrapropionato-1,3-bis(aminomethyl)benzene; Tyr_Z, redox-active tyrosine-161 of the D1 polypeptide; WOC, water oxidizing complex; Y_{ss}, steady-state level kinetics of pulse light photoactivation of O_2 evolution.

S0006-2960(97)00626-0 CCC: $14.00

spin-coupled Mn multimer (Haddy et al., 1992). The line shape of the $g = 4.1$ signal in ammonia-treated PSII samples that are oriented on mylar sheets exhibits resolved Mn hyperfine splitting consistent with at least a dinuclear Mn origin (Kim et al., 1990). Recently, Smith and Pace (1996) identified two forms of the $g = 4.1$ signal that were similar in shape at X-band but showed different line shapes at Q-band. The authors suggested that the four Mn ions are arranged as two exchange-coupled pairs and that each $g = 4.1$ signal arises from a separate Mn dimer.

Washing of the intact WOC with concentrated salt solutions such as $CaCl_2$ releases the 33, 23, and 17 kDa extrinsic WOC proteins [Ono & Inoue, 1983; Murata et al., 1984; Ghanotakis et al., 1984; for a review see Yocum (1991) and Debus (1992)]. Subsequent incubation of these protein-depleted PSII samples leads initially to the release of two of the four Mn ion, interpreted to suggest the presence of two pairs of Mn ions with different chemical affinities [Ono & Inoue, 1983, 1984; Mavankal et al., 1986; for an additional information see Riggs-Gelasco et al. 1996)].

There is much controversy about the proximity of Ca^{2+} to the tetra-Mn cluster. The most extensive information on the organization of the Mn and Ca ions comes from Mn X-ray absorption studies (XAS) by Klein and co-workers (Sauer et al., 1992; Guiles et al., 1990; Yachandra, 1996), George et al., (1989), Penner-Hahn and co-workers (1990), Riggs-Gelasco et al., (1995), Prince et al., (1990) and Kusunoki et al., (1990). The first shell of heavy atom scattering has been assigned to 1.2 ± 0.2 Mn (or possibly Mn and Ca) at 2.7 Å. The identity of the 3.3 Å scattering peak is more controversial. It has been proposed to be due to Ca scattering (0.5−1 atoms) (Yachandra et al., 1996), not to Ca scattering, (Hatch et al., 1995), or to some combination of Mn and light atom scatters (Riggs-Gelasco et al., 1996). According to the Mn EXAFS studies, there is no significant change in the 3.3 Å shell after replacement of Ca^{2+} with Sr^{2+}, Dy^{3+}, or La^{3+}, which has been partly attributed to a Mn−Ca interaction (Yachandra et al., 1993; Riggs-Gelasco et al., 1995). Moreover, Tb^{3+} can displace Ca^{2+} from its binding site in the WOC without prior depletion of the cation or loss of turnover to produce the S_2 state. Yet, it produces no change in the Mn EXAFS, indicating that calcium should be located no closer than 3.6 Å (Hatch et al., 1995). The EXAFS-derived structural model for the $\{Mn_4\}$ core that has emerged from these studies is comprised minimally of two di-μ-oxo dimers (dimer-of-dimers) coupled via a mono-μ-oxo bridge to form a tetra-Mn cluster. Other geometries have been proposed that are also compatible (Yachandra et al., 1996).

Other lines of evidence have supported an interaction between the $\{Mn_4\}$ cluster and Ca^{2+}, either by direct interaction or mediated by the protein. This have been suggested by transformation of the MLS upon Ca^{2+} removal (Boussac & Rutherford, 1988; Boussac et al., 1989; Sivaraja et al., 1989), replacement of Ca^{2+} by Sr^{2+} (Boussac & Rutherford, 1988) and by FTIR spectroscopy (Noguchi et al., 1995).

Competition between Mn^{2+} and other cations, including Ca^{2+}, Mg^{2+} and Na^{+}, during assembly of the WOC by photoactivation has been noted previously in earlier results [Ono & Inoue, 1983; Miller & Brudvig, 1989; for a review see Yocum (1991)]. Divalent cations suppress reoxidation of reduced exogenous electron acceptors like DCIP by Mn^{3+} formed during photoactivation with the following hierarchy: $Ca^{2+} > Sr^{2+} > Ba^{2+} \gg Mg^{2+}$ (Tamura & Cheniae, 1988). This result suggests that calcium and possibly the heavier alkaline earth ions interact with an early photoproduct in the photoactivation process to kinetically or thermodynamically stabilize it against reduction by exogenous reductants. Evidence from thermoluminescence has shown that calcium depletion of the intact WOC stabilizes the WOC against reduction by Q_A^- in the S_2 state (Ono & Inoue, 1989). These data are consistent with the "gatekeeper" role for Ca^{2+} that has been proposed in protecting the $\{Mn_4\}$ cluster via limiting the accessibility of solvent to no more than the two essential substrate water molecules (Tso et al., 1991; Dismukes et al., 1994). It is also known that photoxidation of a protein residue, most probably Tyr_Z, (Gilchrist et al., 1995; Britt, 1996) can be induced on the $S_2 \Rightarrow S_3$ transition in samples having the normal Cl^- cofactor removed or replaced by F^-, even without prior removal of Ca^{2+} (Baumgarten et al., 1990). This result suggests that Ca^{2+} and Cl^- have locations within the WOC that are somehow linked through a common influence on the $Tyr_Z \Leftrightarrow \{Mn_4\}$ interactions.

New insights concerning the structure of the WOC have come from recent studies of photoactivation. Using EPR spectroscopy, equilibrium binding studies have found evidence for the binding of two Mn(II) ions in the dark to the apo-WOC to form a spin-coupled binuclear Mn_2(II,II) pair that can be oxidized by Tyr_Z^+ and can be competed against by other divalent cations (Ananyev & Dismukes, 1995). Also, kinetic analysis of the individual steps of photoactivation showed that at Mn^{2+} concentrations below the dissociation constant for binding, formation of the first intermediate (IM_1) involves ligation and photooxidation of a single Mn^{2+} ion to the apo-WOC (Zaltsman et al., 1997). The following step involves binding of 1 Ca^{2+} in the dark and is the slowest step in photoactivation. This critical step triggers a conformational change in the PSII protein which allows the binding and stable photoxidation of a second Mn^{2+} ion (Ananyev & Dismukes, 1996a,b). The chemical structures of intermediates involved in the reaction of Mn^{2+} with apo-WOC−PSII, depicted as $4Mn^{2+}$ + apo-WOC-PSII $\Rightarrow IM_1...IM_X \Rightarrow \{Mn_4\}$, are unknown.

The present paper addresses this question by revealing conditions which allow the trapping of significant fractions of PSII centers having these intermediates or their precursors present as the dominant equilibrium species. We show that two Mn(II) ions bind in close proximity to form a binuclear Mn_2(II,II) core, and that calcium is required for assembly of this spin-coupled Mn_2(II,II) pair.

MATERIALS AND METHODS

PSII enriched membrane fragments, BBY, were prepared from spinach with a 20:1 of Chl:Triton X-100 ratio (Berthold et al., 1981). Samples at 1 mg of Chl/mL were stored in 10% glycerol at 77 K until they were slowly thawed and washed once in an assay medium containing 300 mM sucrose, 35 mM NaCl, 25 mM MES/NaOH, pH 6.0 buffer. The oxygen evolution rate was 400−500 μmol of O_2/mg of Chl·h under saturated continuous illumination of the untreated PSII membrane fragments with 0.8 mM K_3FeCN_6/1.2 mM DCBQ as electron acceptors.

Manganese and calcium were removed from PSII membrane fragments at 1.0 mg of Chl/mL using the normal assay

medium along with 25−35 mM chelator TPDBA and 1 mM ascorbate, as described earlier (Ananyev & Dismukes, 1995; 1996a). The chelator TPDBA is a bifunctional hydrophobic poly(aminocarboxylate) derivative, ($^{-}$**OOC**−CH_2−CH_2)$_2$=**N**−CH_2−C_6H_4−CH_2−**N**=(CH_2−CH_2−**COO**$^{-}$)$_2$. Each sample of apo-WOC−PSII membrane fragments (BBY membrane fragments after TPDBA treatment) was tested for activity in photoactivation of O_2 evolution as described elsewhere (Ananyev & Dismukes, 1995, 1996a). TPDBA treatment does not remove Chl from PSII membranes (i.e., there is no removal of Mg^{2+} which leads to release of Chl as pheophytin). Concentration of the RC PSII was measured from the photoinduced absorption changes of Pheo at 685 nm with extinction coefficient $\epsilon = 0.32 \times 10^5$ M^{-1} cm^{-1} (Klimov et al., 1982). The residual contamination of Ca^{2+} in apo-WOC-PSII was determined by optical absorption spectroscopy of the Ca^{2+} −arsenazo III complex (sensitivity ≤ 1 μM, $K_D = 60$ μM, and Mg^{2+} artifact at 20 mM) and titration of optical changes at 595 nm by EDTA (Scarpa, 1979). The typical untreated PSII membranes (control samples) and chelator-treated apo-WOC-PSII membranes have residual Ca^{2+} concentration of 10−15 atoms of Ca^{2+}/RC PSII and less than 1 atom of Ca^{2+}/RC PSII, respectively.

Light-induced catalase activity was assayed in a home-built Clark-type O_2 microcell covered with a silicone membrane and loaded with 10 mM H_2O_2 in 25 mM MES-NaOH buffer, pH 6.0; 250 μg of Chl/mL. Sodium azide (0.2 mM) was added to the assay medium to inhibit the heme-iron catalase activity of PSII (Mano et al., 1987). This concentration of NaN_3 was ineffective for inhibition of photoactivation of O_2 evolution (Y_{SS}) at pulse-light illumination. The amplified signal from a precision low-noise current-to-voltage converter and amplifier with adjustable high- and low-frequency filters (model 113 Low-Noise preamplifier, EG&G Princeton Applied Research Corp., U.S.A.) was digitized by using a 12-bit data acquisition interface (WinDaq DI-200 data acquisition) and waveform analysis software for Windows.

The EPR samples were always prepared using dark-incubated (2 h), active (in photoactivation) apo-WOC−PSII membranes at 1 mg of Chl/mL. Concentrated PSII membranes (15 mg of Chl/mL) were collected by centrifugation at 15 000*g* for 4 min and transferred into the bottom of a sealed quartz tube (inner diameter 3 mm) using a special Teflon tube adapter equipped with a nylon piston. Continuous wave EPR spectra were obtained at 9.26 GHz on Bruker ESP 300 spectrometer operating with TE_{102} rectangular cavity with quality factor $Q_L = 8000$ loaded by a sample as described elsewhere (Ananyev & Dismukes, 1995).

Illumination of samples was performed directly in the EPR resonator equipped with eight ultrabright red LED's operated in pulse-light mode (model HPLM 8102 Hewlett Packard). For titration of Tyr_Z^+ by exogenous Mn^{2+}, we used a home-built illuminator to photogenerate Tyr_Z^+ outside of the EPR resonator. It was fabricated using 24 ultrabright red LED's operated in pulse-light mode and arranged symmetrically around a standard quartz EPR tube that was rotated (2 revolution/s) prior to rapid quenching to ≈200 K in a bath of methanol/dry ice.

RESULTS

EPR Signal at g ≈ 8.3 from a Monomeric Mn(II)−Apo-WOC−PSII Center. The chelator treatment of PSII membranes with TPDBA yields apo-WOC−PSII membranes devoid of all manganese and calcium ions required for the expression of WOC activity (Ananyev & Dismukes, 1996a). Figures 1a−c illustrates a portion of the EPR spectra of apo-WOC−PSII membranes in the absence or in the presence of 3 Mn^{2+}/RC added to the medium and recorded in the dark either before or after illumination at 77 K, respectively. The chelator treatment has an additional benefit in that it also removes the EPR signals due to minor contaminating residue of cytochrome b_6, which contains a high-spin heme iron in the region of $g = 6-6.5$. The spectral features in Figure 1 at $g_z \approx 2.96$ and $g_y \approx 2.28$ arise from low potential cytochrome b_{559} (LP), while the peak at $g \sim 4.3$ is due to residual contaminating high-spin ferric iron ($S = {}^5/_2$) that is often found in protein samples. It is noticeable that 30−35 mM TPDBA treatment results in a 16-fold drop in the $g \approx 4.3$ signal of this non-heme iron. EPR reveals that there are no changes in either of these signals upon illumination at

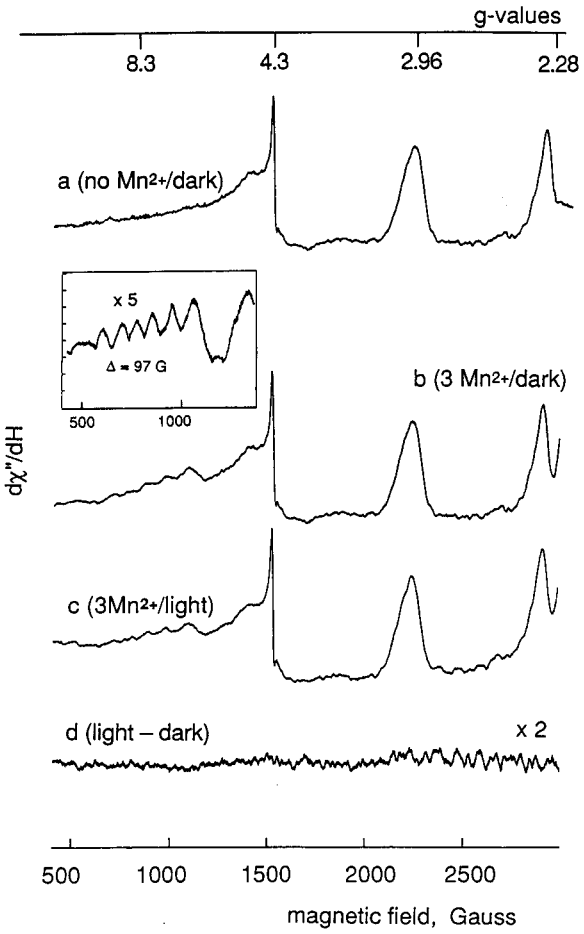

FIGURE 1: EPR spectra of apo-WOC−PSII in the presence of three atoms of Mn^{2+}/RC: (a) apo-WOC−PSII with no Mn^{2+}; (b) apo-WOC−PSII with 3 Mn^{2+}, dark incubation for 10 min before freezing of the sample; (c) apo-WOC-PSII with 3 Mn^{2+} was then illuminated directly inside EPR resonator at 77 K for 5 min; (d) difference between the dark-adapted and illuminated spectra (c *minus* b). Inset shows a 5-fold multiplication of the region $g \approx 8.3$ of six-line signal spectrum (b *minus* a) by re-recording. Assay conditions: apo-WOC-PSII membranes were extracted with 35 mM TPDBA/25 mM MES/NaOH buffer (pH 6.0)/300 mM sucrose. The EPR samples were prepared with photoactivable apo-WOC-PSII membranes that were incubated in the dark for 2 h at 4 °C. EPR conditions: microwave frequency, 9.26 GHz; modulation frequency, 100 kHz; microwave power, 6 dB (51 mW); modulation amplitude, 5 G; sweep time 42 s; each spectrum is an average of 100 scans. Measurements were done at 25 K.

77 K. The chelator treatment was found to transform the high potential cytochrome b_{559} HP to the b_{559} LP form, which results in the absence of a light-induced cytochrome b_{559} signal as the LP form is entirely oxidized by air in the dark. These signals are well understood [for review see Miller and Brudvig (1991)]. The spectrum of apo-WOC−PSII with added Mn^{2+} (Figure 1b; also, see inset) exhibits a previously unreported *set of hyperfine features centered at g ≈ 8.3* that is not found in the apo-WOC−PSII sample (Figure 1a). The average spacing of $\Delta H_{pp} = 94-97$ G identifies this feature as due to Mn^{2+}, while the large apparent *g*-value indicates a site with a relatively strong ligand field with symmetry lower than cubic type (axial or lower). The EPR signal of the LP form of cytochrome b_{559} at $g = 2.96$ can be used for a comparison of signal intensities (1 cytochrome b_{559}/RC). The spectral region near $g \approx 2$ is not shown because this region includes contributions from unbound Mn^{2+}. A figure has been included in the Supporting Information (Figure S1) illustrating the spectrum of apo-WOC−PSII in the presence and absence of added Mn^{2+}. The six-line signal at $g \approx 8.3$ represents only a small fraction of the Mn in the sample.

Illumination at 77 K (Figure 1c and light minus dark spectrum 1d) does not bleach the mononuclear Mn^{2+} signal at $g \approx 8.3$ but does produce small reproducible light-induced changes observable in the range 2100−2900 G. The presence of excess divalent cations like Ca^{2+} or Mg^{2+} (10−20 mM), as well as more than 3 Mn^{2+} atoms/RC, abolish the six-line signal at $g \approx 8.3$ (spectra not shown). This signal is associated with a mononuclear form of Mn^{2+} that is bound to apo-WOC−PSII. The disappearance of the mononuclear Mn^{2+} signal as the divalent cation concentration is increased could be due to several possibilities. It may disappear because of the interaction with one or more additional Mn^{2+} ions, either magnetically, as might occur in a spin-coupled pair, or because of the changing of the binding site as might occur if the protein conformation changes upon binding of additional divalent cations. To investigate the origin of the disappearance of the mononuclear signal at $g \approx 8.3$ upon the presence of Ca^{2+} or Mg^{2+}, we examined the spectral region around $g \approx 2$ where Mn^{2+}, associated with more symmetrical weak ligand fields, can be observed.

Calcium Induces Binding of a Spin-Coupled Dimanganese-(II,II) Center to Apo-WOC−PSII. Figure 2 illustrates the EPR signals for apo-WOC−PSII in the presence of 2 Mn^{2+}/RC added to the medium. Either 10 mM $CaCl_2$ (a) or 10 mM $MgCl_2$ (b) were used. The results show that calcium induces formation of a PSII conformation that can interact with Mn^{2+} to yield a different EPR signal than does Mg^{2+}-treated apo-WOC. The difference spectrum given in Figure 2c reveals the signal arising from Mn^{2+}, which binds to apo-WOC−PSII in the presence of calcium relative to magnesium in the medium. This difference spectrum reveals a broad signal centered near $g \approx 2.04$ ($\Delta H_{pp} = 380 \pm 10$ G) with a shoulder near $g \approx 3.1$. Resolved structure can also be observed on this signal at higher gain. In order to isolate this structure, we subtracted from the original difference spectrum (c) the same spectrum after digital filtering (smoothing) which removes the high frequency components. This double difference spectrum is shown in Figure 2d and reveals a series of at least 11 or more lines with average splitting $\Delta H_{pp} = 42-45$ G. This structure is consistent with the spin-allowed ^{55}Mn hyperfine transitions that are widely found in spin-coupled dimanganese(II,II) centers (Antanaitis et al., 1987; Mathur et al., 1987; Khangulov et al., 1995; Adams et al., 1995).

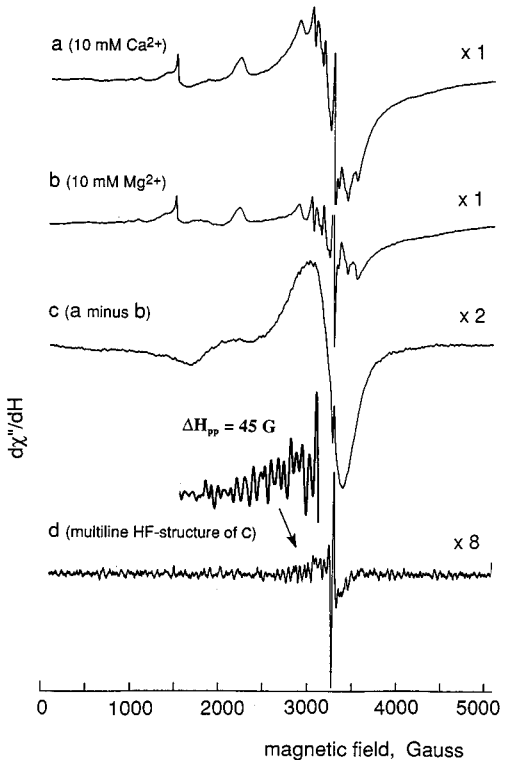

FIGURE 2: EPR spectra illustrating the effect of Ca^{2+} and Mg^{2+} on the binding of 2 atoms of Mn(II)/RC to apo-WOC-PSII in the dark: (a) 10 mM $CaCl_2$/40 mM NaCl, (b) 10 mM $MgCl_2$/40 mM NaCl; (c) spectrum obtained by subtraction (a *minus* b); (d) the difference between original spectrum c and a smoothed spectrum c obtained by digital filtering to remove high-frequency components. (Inset) Expansion of $\Delta H_{pp} = 42-45$ G HF structure from d. Incubation time before freezing was 60 min. The assay and EPR conditions were as in Figure 1. Measurements were done at 25 K.

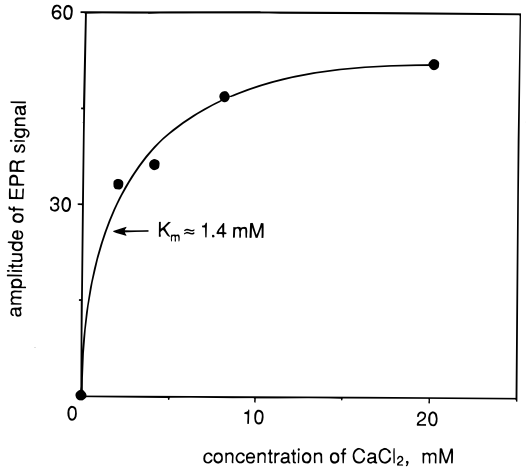

FIGURE 3: Titration of apo-WOC−PSII membranes in the presence of 2 Mn(II)/RC by $CaCl_2$. Free Mn^{2+} and Ca^{2+} were removed by 35 mM bifunctional chelator TPDBA treatment. The amplitude of the broad EPR signal with peak-to-peak separation of 380 ± 10 G (see Figure 2) was plotted as a function of Ca^{2+} concentration. For other experimental details, see the Materials and Methods section and Figure 1 legend.

Figure 3 shows the dependence on $CaCl_2$ concentration in the medium for induction of Mn^{2+} binding to apo-WOC−PSII, plotted as the peak-to-peak amplitude of the 380 G-wide EPR signal from Figure 2c. The samples contain 2 Mn^{2+}/RC added to apo-WOC−PSII. Saturation of Mn^{2+}

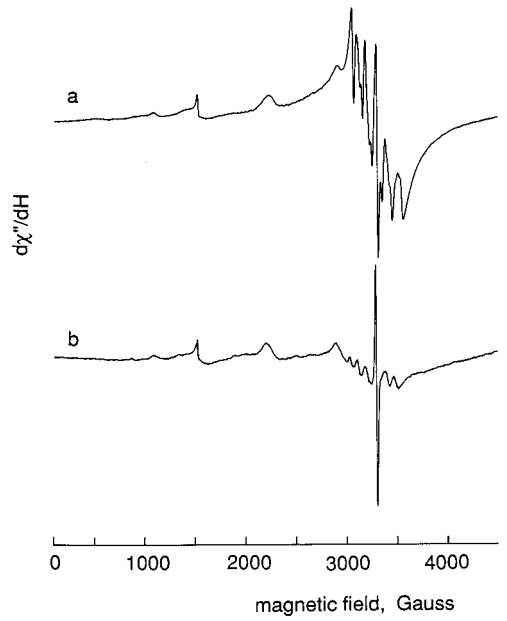

FIGURE 4: Effect of 10 mM $CaCl_2$ washing on the dark ligation of added Mn(II) with apo-WOC-PSII membranes: (a) apo-WOC-PSII membranes (1 mg of Chl/mL) were incubated with 250 μM $MnCl_2$ and washed 3 times (centrifugation at 14000*g*, 4 min) in an excess of the assay medium containing no Mn^{2+} or Ca^{2+}; (b) sample was prepared identically to a except that 10 mM $CaCl_2$ was added to the assay medium prior to the second centrifugation and after removal of unbound Mn(II) on the first centrifugation/washing cycle. The sample was washed/centrifuged a third time in the assay medium without Mn^{2+} or Ca^{2+}. Assay medium contains: 300 mM sucrose, 35 mM NaCl, 25 mM MES/NaOH, pH 6.0 buffer. EPR conditions: microwave frequency, 9.26 GHz; modulation frequency, 100 kHz; microwave power, 24 dB (0.81 mW); modulation amplitude, 5 G; sweep time 42 s; each spectrum is an average of 10 scans. Measurements were done at 25 K.

binding occurs at *ca.* 10 mM $CaCl_2$, with an apparent dissociation constant for Ca^{2+} induction of the Mn^{2+} EPR signal of 1.4 mM (see Figure 3). This calcium dissociation constant has the same value as the one found for the Michaelis constant for calcium activation of O_2 evolution [reviewed by Yocum (1991) and Debus (1992)]. In addition, the Michaelis constant for calcium induction of binding and photooxidation of the second Mn^{2+} ion is required during assembly of the WOC by photoactivation of O_2 evolution (Zaltsman et al., 1997).

Apo-WOC−PSII membranes will also bind Mn^{2+} ions with low affinity to nonspecific sites if high concentrations of $MnCl_2$ are used well above stoichiometric levels and in the absence of other divalent ions. This binding is easily monitored by EPR as the appearance of a strong six-line signal at $g \approx 2$ from bound or trapped Mn^{2+} that is not released by repeated washing in buffers lacking salts (Figure 4a). However, this signal is readily abolished by excess divalent cations like Ca^{2+} or Mg^{2+} with equal effectiveness on a single wash (Figure 4b). This effect is due to the release of Mn^{2+} instead of an ionic strength effect on signal amplitude. Calcium has been previously found to prevent or reverse the binding of this low affinity nonfunctional $Mn^{\geq 2+}$ (Chen et al., 1995).

Tyr_Z^+ Oxidizes the Calcium-Induced Mn_2^{II} Core in PSII with a Higher Quantum Yield than the High-Affinity Mn(II) Site. Previous studies have shown that Tyr_Z^+ oxidizes Mn-(II) at a high-affinity site on apo-WOC−PSII (Klimov et al., 1982; Hoganson et al., 1989; Blubaugh & Cheniae, 1992).

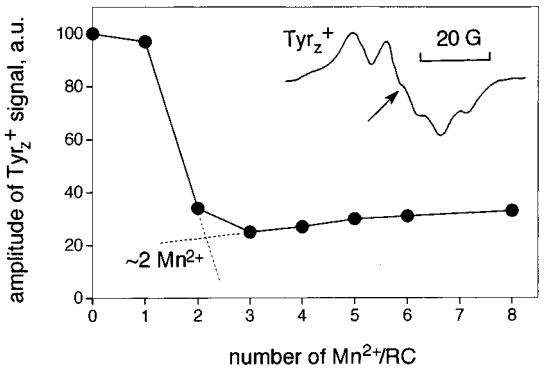

FIGURE 5: Titration of Tyr_Z^+ (light *minus* dark EPR spectrum) in apo-WOC-PSII membranes by exogenic Mn(II). The magnitude of the Tyr_Z^+ signal induced by 8 light pulses at 293 K was plotted as a function of the number of Mn(II) per RC after subtraction of Tyr_D^+ in the dark control sample. (Inset) Spectrum of light−dark Tyr_Z^+ EPR signal (temperature, 25 K; microwave power, 2.4 μW; modulation amplitude, 2 G). The sample of apo-WOC-PSII membranes (2.5 mg of Chl/mL, 10 mM $CaCl_2$, and 2 mM K_3FeCN_6) was positioned inside a rotating (two revolutions/s) standard EPR quartz tube. The sample was illuminated by 24 ultrabright red HPLM 8102 LED's (duration of light period, $t_{light} = 40$ ms, and duration of dark period, $t_{dark} = 2$ s) and quickly frozen in a methanol/dry ice bath after the last (eighth) light pulse. EPR conditions: microwave power, 3.2 mW; modulation amplitude, 2 G; sweep time 42 s; each spectrum is an average of 5 scans. Measurements were done at 25 K.

To determine if the calcium-induced Mn_2(II,II) core of PSII could act as a functional electron donor to Tyr_Z^+ we examined the yield of the light-induced Tyr_Z^+ EPR signal as a function of the number of Mn^{2+} per RC PSII, as shown in Figure 5. The calcium concentration and conditions (other than Mn^{2+} concentration) were fixed to optimize formation of the dark Mn_2^{II}−PSII center (Figure 2c). The sample was illuminated at 293 K and quickly frozen after the last flash in a series of flashes as described in the legend. The flashes were chosen so that they produce the maximum conversion to the first light-induced intermediate formed during photoactivation at room temperature, i.e., stopped at the end of the kinetic lag phase in recovery of O_2 production and prior to formation of the second photooxidized intermediate (Ananyev & Dismukes, 1996a; Zaltsman et al., 1997). Under these conditions, the amplitude of the flash-induced Tyr_Z^+ signal strongly depends on the number of added Mn^{2+} ions per RC. As shown in Figure 5, in the presence of one Mn^{2+}/RC, there is a small loss in the Tyr_Z^+ signal in comparison with the sample where no Mn^{2+} is added (less than 5%). However, addition of only two Mn^{2+}/RC decreases the amplitude to 35% of the initial Tyr_Z^+ signal, while further increase in Mn^{2+} concentration to 3 Mn/RC causes a smaller decrease by less than 10%. Further addition of Mn does not produce more effective reduction of Tyr_Z^+. This decrease in the light-induced yield of Tyr_Z^+ in the presence of two Mn^{2+} occurs only if Ca^{2+} is present at concentrations which produce the spin-coupled Mn_2(II,II) signal at $g = 2.04$. The samples contain no exogenous electron acceptor such that the number of photolytic turnovers is limited by the residual plastoquinone pool. These results indicate that the quantum yield for reduction of photooxidized Tyr_Z^+ by added Mn^{2+} is greatly increased upon binding of a second ion of Mn^{2+}, at calcium concentrations which optimize formation in the dark of the spin-coupled Mn_2^{II}−PSII core.

These results are supported by earlier work by Klimov et al. (1982), who showed that a maximum yield in variable

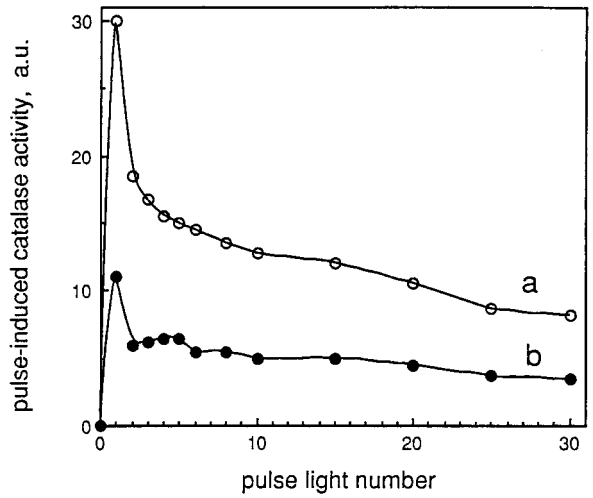

FIGURE 6: Effect of exogenous Mn^{2+} and Ca^{2+} on apo-WOC-PSII catalase activity measured as the oxygen yield from H_2O_2 per flash as a function of the number of single-turnover xenon flashes (4 μs FWHM, given at 0.2 Hz). Sample of apo-WOC−PSII membranes (250 μg of Chl/mL) in the presence of 200 μM NaN_3 and 10 mM H_2O_2: (a) the difference in catalase activity between [apo-PSII + 8Mn(II)] *minus* [apo-PSII]; (b) the difference in catalase activity between [apo-PSII + 8Mn(II) + 8mM Ca^{2+}] *minus* [apo-PSII]. No exogenous electron acceptor was added.

fluorescence, ΔF, is observed from apo-WOC−PSII fragments, following the addition of 2 Mn/RC. Also, time-resolved EPR measurements of the lifetime of Tyr_Z^+ previously have shown that Mn^{2+} directly reduces Tyr_Z^+ (Hoganson et al., 1989). The influence of calcium on the efficiency of electron donation by Mn^{2+} was not previously reported.

Effect of Ca^{2+} on Single-Turnover Flash-Induced Catalase Activity. Inoue and Wada (1987) found that Mn(II)-catalyzed photooxidation of H_2O_2 by Tris-treated PSII (non-photoactivable) was strongly inhibited by 1 mM Ca^{2+} or Mg^{2+}. In this section we developed the investigations using photoactivable apo-PSII and single-turnover flashes. Under these conditions, the metalloenzyme complex of Mn(II) with apo-PSII exhibit a catalase activity (Figure 6). Mn-dependent catalase activity of apo-PSII is difficult to study because there exists some heme iron dependent residual catalase activity. For elimination of this kind of catalase activity we used 0.2 mM NaN_3 (Mano et al., 1987). Our additional data shows that no significant changes occur in the kinetics of photoactivation of O_2 evolution in the presence of 0.2 mM NaN_3.

The upper curve in Figure 6 demonstrates the catalase activity of TPDBA-treated apo-PSII in the presence of Mn^{2+}. This activity is maximal at the first flash demonstrating a one-flash requirement (one-quantum process of H_2O_2 dependent O_2 evolution) and steadily decreases with each following flash. The drop in the catalase activity is caused by the depletion of electron-accepting capacity of PSII. The lower curve (Figure 6b) represents the catalase activity in the presence of both Mn^{2+} and Ca^{2+}. It clearly demonstrates that Ca^{2+} inhibits the activity by *ca.* 60%. These results support our suggestion that Ca^{2+} modulates the accessibility or reactivity of the Mn_2(II,II) site with H_2O_2.

DISCUSSION

Detection of an EPR Signal for a High-Affinity Monomeric Mn^{2+}−PSII Center. From the data in Figure 1, we can conclude that in the absence of added $CaCl_2$ there is a monomeric Mn^{2+} binding site in apo-WOC−PSII that is characterized by a six-line EPR signal centered at an apparent g value of 8.3. Due to the interference from other EPR signals, it is not evident where the other zero-field transitions expected for this monomeric Mn^{2+} center are located in the spectrum. Hence, a quantitative estimate of the zero-field splitting is not yet possible. However, such large apparent g values suggest an unsymmetrical ligand field of noncubic symmetry (Markham, 1986; Reed, 1986; Aasa et al., 1987). It is not clear how to identify this site, but it appears to be attributable to the high-affinity Mn^{2+} binding site implicated in electron transfer to Tyr_z^+, rather than to the Ca^{2+} binding site [for review see Yocum (1991) and Debus (1992)]. We suggest that the six-line EPR signal centered in the $g \approx 8.3$ region represents the monomeric Mn(II) form in the first step during assembly of the Mn_2^{II} core of the functional $\{Mn_4\}$ cluster. This complex of the monomeric Mn(II) with apo-WOC−PSII exhibits a large barrier to photooxidation at 77 K, but can be photooxidized at room temperature.

Previously, Rutherford's group (Booth et al., 1996) demonstrated that when stoichiometric amounts of Mn^{2+} ions are added to Ca^{2+}-depleted PSII, the six-line pattern of aqua Mn(II) ions is not detected. Thus, we may attribute the Mn^{2+} EPR signal at $g \approx 8.3$ that forms upon binding of exogenous Mn^{2+} to apo-WOC−PSII, seen in the present work, to the loss of aqua Mn^{2+} in the presence of Ca-depleted PSII reported by Booth et al. (1996). We also see a loss of the aqua Mn(II) EPR signal in the presence of apo-WOC−PSII. However, detection of the bound Mn(II) signal at $g \approx 8.3$ requires PSII samples that lack all residual Mn^{2+} and Ca^{2+}, as well as contamination by adventitious Fe^{3+}. The hydrophobic chelator TPBDA has proven to be the most effective chelator we have found for this purpose.

Origin of the Calcium-Induced Dimanganese(II,II) EPR Signal. The data in Figures 2, 3, and 5 provide a self-consistent set of observations, showing that calcium induces a conformation of the apo-WOC−PSII protein which is capable of binding Mn^{2+} with higher affinity that occurs in the absence of calcium. Moreover, the g value, broad lineshape, and the resolved hyperfine structure of this EPR signal are very similar to that observed in a number of examples of weakly interacting Mn^{2+} pairs that are coupled by weak electron spin-exchange and magnetic dipolar terms (Weltner, 1983; Khangulov et al., 1995). Examples of Mn_2^{II} centers with spectra almost identical to those in Figure 2c include pairs in which the Mn(II) ions are separated by a relatively large distance (R): Mn(II)-substituted concanavalin A (R = 4.2 Å; Antanaitis et al., 1987), xylose isomerase (R = 4.9 Å; Whitlow et al., 1991), and a dinuclear (μ-carboxylato)manganese(II) complex (R = 4.9 Å; Adams et al., 1995). In each of these cases, the Mn(II) ions are bridged by carboxylate anions which coordinate via the anti-lone pairs of each of the two carboxylate O atoms. Such a long separation produces relatively weak zero-field splitting of the EPR signal. The EPR line shapes in these complexes and in Figure 2c do not fall into the class of strong zero-field split spectra such as those observed with short inter-manganese separations, common in complexes with single-atom bridges (O^{2-}, OH^-, OR^-, halides; R = 2.9−3.5 Å). On this basis, we suggest that the calcum-induced folding of PSII, which creates the binding site for the Mn_2^{II} core, may include a carboxylate bridge between the Mn(II) ions and that the Mn(II) ions are separated by 3.7−4.5 Å

Scheme 1: Model for Binding to the D1 Protein and Photoxidation of Mn_2(II,II) Core in the First Steps of the Assembly of the Active Center WOC[a]

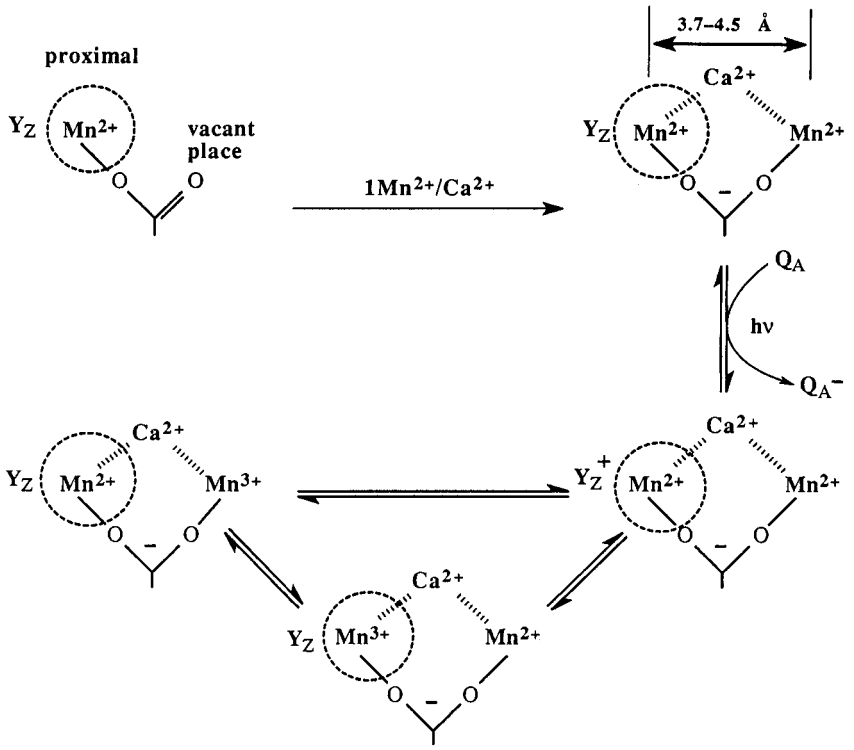

[a] The dashed lines imply that bridging anions such as Cl^-, OH^-, or $-COO^-$ are bound between $Mn^{2+,3+}$ and Ca^{2+}.

Chart 1: EPR-Derived Model for Ca-Induced Binuclear Mn_2(II,II) Core in Apo-WOC−PSII

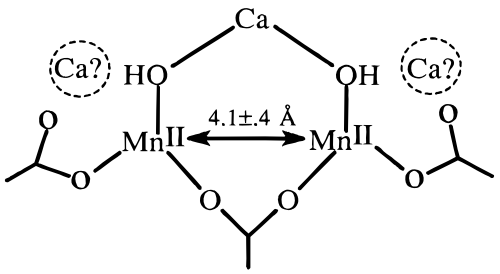

Chart 2: Proposed Speculative Model for the Photosynthetic Tetramanganese Cluster of the WOC in the S1 State Based on Extrapolation of the EPR Model and Mn EXAFS Data (Yachandra et al., 1993)

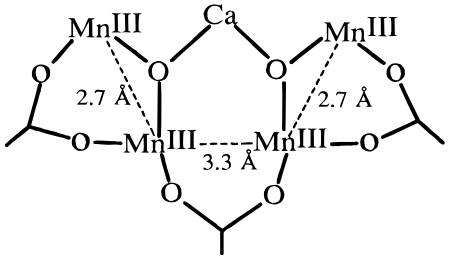

(Scheme 1 and Chart 1). The lower limit is based on the assignment of the shoulder at $g \approx 3.1$ to zero-field splitting of two $S = 5/2$ ions. We note that involvement of a protein-derived carboxylate has also been suggested in the initial step of photoactivation (Tamura et al., 1989; Blubaugh & Cheniae, 1992).

It is also conceivable, although unlikely, that the resolved structure on top of the broad signal may arise from spin-forbidden ^{55}Mn hyperfine transitions that sometimes occur in rare situations of mononuclear Mn^{2+} centers having large zero-field splitting produced by a strongly distorted rhombohedral ligand field (Abragam & Bleaney, 1970). However, there are no other zero-field transitions observed in the spectrum of the Ca-induced Mn_2(II,II) signal, as would be required for such a ligand field. Hence, we exclude this interpretation.

We propose that calcium organizes the binding site for Mn ions in the apo-WOC protein and may even interact closely with the Mn_2(II,II) pair by solvent or protein-derived bridging ligands. A speculative structure for this Ca-induced Mn_2(II,II) center is shown as Chart 1. Chart 1 is also consistent with the Mn_2(μ-oxo)(μ-carboxylate) core proposed by Semin and Parak (1997) on the basis of sequence homology between the D1 and D2 reaction center polypeptides and other O_2 activating proteins: methane monooxygenase and ribonucleotide reductase. There may be Cl^- ions associated with this intermediate, but we have not completed the studies needed to establish this possibility. We have presented evidence that this species can be photooxidized to yield a species equivalent to IM_2, the second light-induced intermediate in photoactivation. Two more Mn^{2+} ions bind to this intermediate in steps which are faster and probably do not require additional Ca ions. We further speculate that a possible structure for the S1 oxidation state could involve a tetrameric Mn(III) species, such as the minimal structure depicted as Chart 2.

This speculative tetrameric model could be obtained from the Mn_2(II,II) precursor by binding and photoxidation of two Mn^{2+} ions to terminal hydroxide sites by deprotonation to form triply bridging μ_3-oxo atoms between end pairs of Mn ions and Ca. The resulting Mn tetramer can be viewed as two copies of mono-μ_3-oxo bridged Mn_2Ca trimers that are fused together by sharing a common Ca ion.

According to Figure 5, when two atoms of Mn^{2+} are allowed to bind to this calcium-induced site in PSII, the Mn_2^{II} center that forms exhibits a considerably higher quantum yield for the reduction of Tyr_Z^+ than for that observed with only one Mn^{2+} present. In Scheme 1 we suggest an explanation for this phenomenon in terms of a reduced rate of charge recombination. A slower rate of charge recombination would be expected if intramanganese electron transfer occurs between the "gateway" Mn^{3+} ion located at the proximal site closest to Tyr_Z and the second Mn^{2+} ion in the Mn_2^{II} pair, termed here the distal Mn site. This electron transfer step could further separate and/or stabilize the electron-hole pair against recombination, thereby producing a lower yield of oxidized Tyr_Z^+. We suggest that this "gateway" Mn site is identical to the "gateway" Mn site observed in the intact WOC, which is responsible for mediating electron transfer between the remaining three Mn ions and Tyr_Z (Dismukes et al., 1994).

Relationship to Intermediates Formed During Photoactivation. It is necessary to understand how the calcium-induced Mn_2^{II} core fits into the scheme for assembly of the tetramanganese active site of the WOC by photoactivation. In previous works, determination of the reaction orders (molecularities) with respect to Mn^{2+}, Ca^{2+}, and H^+ concentrations in the first two steps of photoactivation have found that (1) one atom of Mn^{2+} binds to apo-WOC−PSII and is photoxidized with concurrent displacement of a weakly bound nonfunctional Ca^{2+} ion on the first light-induced step; (2) this step is followed by the slowest step in photoactivation, the binding of one Ca^{2+} ion to the first intermediate (Mn^{3+}−WOC−PSII) *via* a slow conformational change in the structure of PSII, prior to binding and photooxidation of a second Mn^{2+} that yields the metastable intermediate IM_2; (3) a proton is released into solution either on the first photolytic step or upon subsequent binding of Ca^{2+} in the dark (Ananyev & Dismukes, 1996a,b; Zaltsman et al., 1997).

The photoactivation experiments described above were performed at low concentration of Mn (micromolar) conditions very different from the present studies, and so thus involve different initial states of Mn association. Quantitative removal of all Mn in the starting material was independently established. Under the low apo-WOC−PSII (1 μM P680) and Mn^{2+} (0.25−20 μM) concentrations used for the photoactivation experiments (saturating calcium levels, 8−10 mM), we observed that the initial species in the dark are Ca^{2+}−apo-WOC−PSII and free (unbound) Mn^{2+} in solution. Consequently, the metastable intermediate IM_2 is formulated as comprised of 2 Mn(III) ions and at least one essential Ca^{2+}. The Mn stoichiometry of two agrees exactly with the result found here for the calcium-induced dimanganese(II,-II) site, which is bound in the dark before photolysis. Under the low RC and Mn concentration used for photoactivation, the high affinity Mn site ($K_D = 10\ \mu$M) will not be occupied, in contrast to the EPR studies reported here, which were performed at 100−120 μM Mn^{2+} and 50−60 μM RC, conditions which lead to complete saturation of the high affinity Mn site. We can therefore assign the photoactivation intermediate IM_2 as probably representing the doubly oxidized product of the calcium-induced spin-coupled Mn_2^{II} center that binds in the dark in the presence of calcium.

ACKNOWLEDGMENT

The authors thank Drs. S. Khangulov, A. Boelrijk, M. Zheng, and, especially, Ms. L. Zaltsman for useful discussions during experimentation and preparation of the article. We are also grateful to Professors N. Tamura and A.-F. Miller for providing useful advice.

SUPPORTING INFORMATION AVAILABLE

Experimental recording of a $g = 2$ region of EPR spectra (2 pages). Ordering information is given on any current masthead page.

REFERENCES

Aasa, R., Andreasson, L.-E., Lagenfelt, G., & Vanngard, T. (1987) *FEBS Lett. 221*, 245−248.
Abragam, A., & Bleaney, B. (1970) *Electron Paramagnetic Resonance of Transition Ions*, Oxford University Press, London.
Adams, H., Bailey, N. A., Debaecker, N., Fenton, D. E., Kanda, W., Latour, J.-M., Okawa, H., & Sakiyama, H. (1995) *Angew. Chem., Int. Ed. Engl. 34*, 535−537.
Ahrling, K. A., & Pace, R. J. (1995) *Biophys. J. 68*, 2081−2090.
Ananyev, G. M., & Dismukes, G. C. (1995) in *Photosynthesis: From Light to Biosphere* (Mathis, P., Ed.) Vol. 2, pp 431−434, Kluwer Academic Publishers, Dordrecht, The Netherlands.
Ananyev, G. M., & Dismukes, G. C. (1996a) *Biochemistry 35*, 4102−4109.
Ananyev, G. M., & Dismukes, G. C. (1996b) *Biochemistry 35*, 14608−14617.
Antanaitis, B. C., Brown III, R. D., Chasteen, N. D., Freedman, J. H., Koenig, S. H., Lilienthal, H. R., Peisach, J., & Brewer, C. F. (1987) *Biochemistry 26*, 7932−7937.
Baumgarten, M., Philo, J. S., & Dismukes, G. C. (1990) *Biochemistry 29*, 10814−10822.
Berthold, D. A., Babcock, G. T., & Yocum, C. F. (1981) *FEBS Lett. 134*, 231−234.
Blubaugh, D. J., & Cheniae, G. M. (1992) in *Research in Photosynthesis* (Murata, N., Ed.) Vol. 2, pp 361−364, Kluwer Academic Publishers, Dordrecht, The Netherlands.
Bonvoisin, J., Blondin, G., Girerd, J. J., & Zimmermann, J. L. (1992) *Biophys. J. 61*, 1076−1086.
Booth, P. J., Rutherford, A. W., & Boussac, A. (1996) *Biochim. Biophys. Acta 1277*, 127−134.
Boussac, A., & Rutherford, A. W. (1988) *Biochemistry 27*, 3476−3483.
Boussac, A., Zimmermann, J. L., & Rutherford, A. W. (1989) *Biochemistry 28*, 8994−8989.
Boussac, A., Girerd, J. J., & Rutherford, A. W. (1996) *Biochemistry 35*, 6984−6989.
Britt, R. D. (1996) in *Oxygenic Photosynthesis: The Light Reactions* (Ort, D. R., & Yocum, C. F., Eds.) pp 137−164, Kluwer Academic Publishers, Dordrecht, The Netherlands.
Casey, J., & Sauer, K. (1984) *Biochim. Biophys. Acta 767*, 21−28.
Chen, C., Kazimir, J., & Cheniae, G. M. (1995) *Biochemistry 34*, 13511−13526.
Debus, R. J. (1992) *Biochim. Biophys. Acta 1102*, 269−353.
dePaula, J. C., & Brudvig, G. (1985) *J. Am. Chem. Soc. 107*, 2643−2648.
dePaula, J. C., Beck, W. F., & Brudvig, G. W. (1986) *J. Am. Chem. Soc. 108*, 4002−4008.
Dismukes, G. C. (1991) in *Mixed Valency Systems: Applications in Chemistry, Physics and Biology* (Prassides, K, Ed.) pp 137−154, Kluwer Academic Publishers, Dordrecht, The Netherlands.
Dismukes, G. C., Ferris, K., & Watnick, P. (1982) *Photobiochem. Photobiophys. 3*, 243−248.
Dismukes, G. C., Zheng, M., Hutchins, R., & Philo, J. S. (1994) *The Inorganic Biochemistry of Photosynthetic Water Oxidation*, Vol. 22, No. 2, pp 323−327, The Biochemical Society, London.
George, G. N., Prince, R. C., & Cramer, C. P. (1989) *Science 243*, 789−791.
Ghanotakis, D. F., Topper, J. N., & Yocum, C. F. (1984) *Biochim. Biophys. Acta 767*, 524−531.

Gilchrist, M. L., Ball, J. A., Randall, D. W., & Britt, D (1995) *Proc. Natl. Acad. Sci. U.S.A. 92*, 9545−9549.
Guiles, R. D., Zimmermann, J.-L., McDermott, A. E., Yachandra, V. K., Cole, J. L., Dexheimer, S. L., Britt, R. D., Wieghardt, K., Bossek, U., Sauer, K., & Klein, M. P. (1990) *Biochemistry 29*, 471−485.
Haddy, A., Dunham, W. R., Sands, R. H., & Aasa, R. (1992) *Biochim. Biophys. Acta 1099*, 25−34.
Hatch, C., Grush, M., Bradley, R., LoBrutto, R., Cramer, S., & Frasch, W. (1995) in *Photosynthesis: From Light to Biosphere* (Mathis, P., Ed.) Vol. 2, pp 425−429, Kluwer Academic Publishers, Dordrecht, The Netherlands.
Hoganson, C. W., Ghanotakis, D. F., Babcock, G. T., & Yocum, C. F. (1989) *Photosynth. Res. 22*, 285−293.
Inoue, H., & Wada, T. (1987) *Plant Cell Physiol. 28*, 767−763.
Khangulov, S. V., Pessiki, P. J., Barynin, V. V., Ash, D. E., & Dismukes, G. C. (1995) *Biochemistry 34*, 2015−2025.
Kim, D. F., Britt, R. D., Klein, M. P., & Sauer, K. (1990) *J. Am. Chem. Soc. 112*, 541−547.
Klimov, V. V., Allakhverdiev, S. I., Shuvalov, V. A., & Krasnovsky, A. A. (1982) *FEBS Lett. 148*, 307−312.
Kusunoki, M. (1992) *Chem. Phys. Lett. 197*,108−116.
Kusunoki, M., Ono, T.-A., Marsushita, T., Oyanagi, H., & Inoue, Y. (1990) *J. Biochem. 108*, 560−567.
Lei, J. R., & Kramer, M. A. (1988) *ACM Trans. Math. Software 14*, 61−67.
Mano, J., Takahashi, M., & Asada, K. (1987) *Biochemistry 26*, 2495−2501.
Markham, G. D. (1986) in *Manganese in Metabolism and Enzyme Function* (Schramm, V. L., & Wedler, F. C., Eds.) pp 379−403, Academic Press, New York.
Mathur, P., Crowder, M., & Dismukes, G. C. (1987) *J. Am. Chem. Soc. 109*, 5527−5232.
Mavankal, G., McCain, D. C., & Bricker, T. M. (1986) *FEBS Lett. 202*, 235−239.
Miller, A.-F., & Brudvig G. W. (1989) *Biochemistry 28*, 8181−8190.
Miller, A.-F., & Brudvig, G. W. (1991) *Biochim. Biophys. Acta 1056*, 1−18.
Murata, N., Miyao, M., Omata, T., Matsunami, H., & Kuwabara, T. (1984) *Biochim. Biophys. Acta 765*, 363−369.
Noguchi, T., Ono, T.-A., & Inoue, Y. (1995) *Biochim. Biophys. Acta 1228*, 189−200.
Ono, T. A., & Inoue, Y. (1983a) in *The Oxygen Evolving System of Photosynthesis* (Inoue, Y., et al., Eds.) pp 337−344, Academic Press Japan, Tokyo.
Ono, T.-A., & Inoue, Y. (1983b) *FEBS Lett. 164*, 255−260.
Ono, T.-A., & Inoue, Y. (1984) *FEBS Lett. 168*, 281−286.
Ono, T.-A., & Inoue, Y. (1989) *Arch. Biochem. Biophys. 275*, 440−448.
Penner-Hahn, J. E., Fronko, R. H., Pecoraro, V. L., Yocum, C. F., Betts, S. D., & Bowlby, N. R. (1990) *J. Am. Chem. Soc. 112*, 2549−2557.
Prince, R. C., Cramer, S. P., & George, G. N. (1990) in *Current Research in Photosynthesis* (Baltscheffsky, M., Ed.) Vol. 1, pp 685−692, Kluwer Academic Press, Dordrecht, The Netherlands.
Randall, D. W., Sturgeon, B. E., Ball, J. A., Lorigan, G. A., Chan, M. K., Klein, M. P., Armstrong, W. H., & Britt, R. D. (1995) *J. Am. Chem. Soc. 117* (51), 11780.
Reed, G. H. (1986) in *Manganese in Metabolism and Enzyme Function* (Schramm, V. L., & Wedler, F. C. Eds.) pp 313−323, Academic Press, New York.
Riggs-Gelasco, P. J., Mei, R., & Penner-Hahn, J. E. (1995) *Adv. Chem. Ser. 246*, 219-248.
Riggs-Gelasco, P. J., Mei, R., Ghanotakis, D. F., Yocum, C. F., & Penner-Hahn, J. E. (1996) *J. Am. Chem. Soc. 118*, 2400−2410.
Sauer, K., Yachandra, V. K., Britt, R. D., & Klein, M. P. (1992) in *Manganese Redox Enzymes* (Pecoraro, V. L., Ed.) pp 141−176, VCH Publishers, New York.
Scarpa, A. (1979) in *Methods in Enzymology* (Fleischer, S., & Packer, L., Eds.) pp 301−338, Academic Press, Inc., New York.
Semin, B. K., & Parak, F. (1997) *FEBS Lett. 400*, 259−262.
Sivaraja, M., Tso, J., & Dismukes, G. C. (1989) *Biochemistry 28*, 9459−9464.
Smith, P. J., & Pace, R. J. (1996) *Biochim. Biophys. Acta 1275*, 213−220.
Tamura, N., & Cheniae, G. M. (1988) in *Light-Energy Transduction in Photosynthesis: Higher Plants and Bacterial Models* (Stevens, S. E., & Bryant, D. A., Eds.) pp 227−242, The American Society of Plant Physiologists, Rockville, MD.
Tamura, N., Ikeuchi, M., & Inoue, Y. (1989) *Biochim. Biophys. Acta 973*, 228−236.
Tso, J., Sivaraja, M., & Dismukes, G. C. (1991) *Biochemistry 30*, 4734−4739.
Weltner, W. (1983) *Magnetic Atoms and Molecules*, Dover Publications Inc., New York.
Whitlow, M., Howard, H. J., Finzel, B. C., Foulos, T. L., Winborne, E., & Gilliland, G. L. (1991) *Proteins 9*, 153−173.
Yachandra, V. K., DeRose, V. J., Latimer, M. J., Mukerji, I., Sauer, K., & Klein, M. P. (1993) *Science 260*, 675−679.
Yachandra, V. K., Sauer, K., & Klein, M. P. (1996) *Chem. Rev. 96*, 2927−2950.
Yocum, C. F. (1991) *Biochim. Biophys. Acta 1059*, 1−15.
Zaltsman, L., Ananyev G. M., Bruntrager, T., & Dismukes, G. C. (1997) *Biochemistry 36*, 8914−8922.
Zheng, M., & Dismukes, G. C. (1996) *Inorg. Chem. 35*, 3307−3319.
Zimmermann, J.-L., & Rutherford, A. W. (1984) *Biochim. Biophys. Acta 767*, 160−170.
Zimmermann, J.-L., & Rutherford, A. W. (1986) *Biochemistry 25*, 4609−4615.

BI970626A